Nanoscale Coherent Light Source

Raphael Holzinger,[*] David Plankensteiner, Laurin Ostermann, and Helmut Ritsch

Institut für Theoretische Physik, Universität Innsbruck, Technikerstraße 21a, A-6020 Innsbruck, Austria

A laser is composed of an optical resonator and a gain medium. When stimulated emission dominates mirror losses, the emitted light becomes coherent. We propose a new class of coherent light sources based on wavelength sized regular structures of quantum emitters whose eigenmodes form high-Q resonators. Incoherent pumping of few atoms induces light emission with spatial and temporal coherence. We show that an atomic nanoring with a single gain atom at the center behaves like a thresholdless laser, featuring a narrow linewidth. Symmetric subradiant excitations provide optimal operating conditions.

Introduction.—Conventional lasers consist of an optical cavity filled with a gain medium, typically comprised of an ensemble of energetically inverted emitters amplifying the light field via stimulated emission. Pioneering experiments have realized lasers with the most minimalistic gain medium yet, a single atom [1–8]. Corresponding theoretical quantum models have been studied extensively for several decades [9–12]. Any standard model of a laser, however, still features a macroscopic optical resonator supporting the corresponding laser light mode. Technically, the noise of the cavity mirrors is a substantially limiting factor for the frequency stability of a laser. This can be reduced when working in the bad cavity regime, such that the coherence is stored in the atomic dipoles rather than the light field. In such superradiant lasers [13–17], the properties of the emitted light are governed by the gain medium rather than the resonator.

In this work, we go one step further, removing the cavity altogether, and consider a nanoscale system. Atomic quantum emitters provide for the necessary gain while simultaneously acting as a resonator, when they are partially illuminated by incoherent light. In principle, the size of the entire setup can be reduced to even below the order of the laser wavelength. On top of this, its performance is fully determined by the spectral properties of the atomic medium. Since the atoms behave as a collective, the single-atom spectral features do not constitute a fundamental limit. Thus, as we will show, the output light can have a coherence time larger than that of a single atom.

As discovered recently, tailored dipole-coupled atomic arrays possess collective eigenmodes with a very long lifetime demonstrating analogous characteristics to a high-Q optical cavity mode [18–20]. Such arrangements could be implemented, e.g., by means of optical tweezers [21–23] or superconducting qubit setups operating in the microwave regime [24]. We study the prospects of implementing a minimalistic subwavelength sized laser. As our generic setup, we consider a single atom placed in the center of a small ring comprised of identical emitters. The collective couplings are mediated by virtual photon exchange through the electromagnetic vacuum [6,25,26]. The eigenstates of the outer ring take on the role of a resonator mode.

We show that such a minimal model constitutes a steady-state coherent light source with a spectral linewidth well
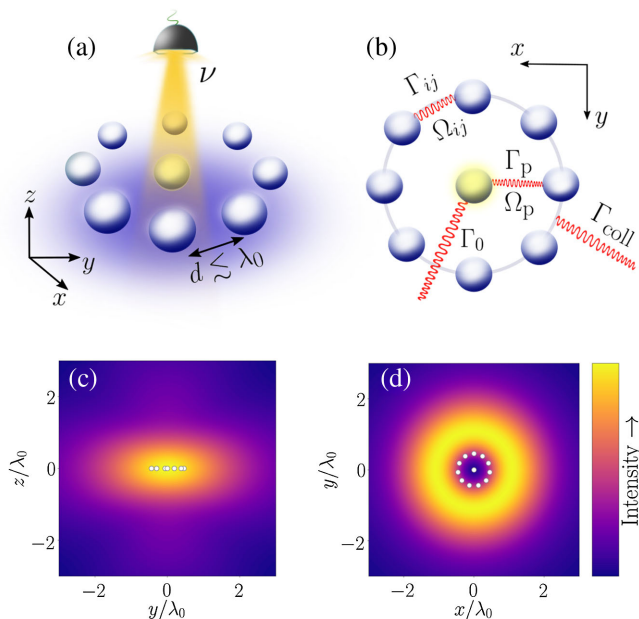

FIG. 1. Coherent light emission from a partially pumped atomic array. (a) A ring of atoms with an additional atom in its center incoherently pumped with a rate ν. (b) The atoms decay at a spontaneous decay rate Γ_0 and are collectively coupled to the center atom with dispersive coupling Ω_p and dissipative coupling Γ_p, respectively. In turn, the ring atoms have couplings Ω_{ij} and Γ_{ij} among each other. The symmetric excitation exhibits a collective decay rate Γ_{coll}. (c) The field intensity generated in the steady state according to Eq. (3) for a ring of $N = 11$ atoms in the xz plane with $y = 2.5\lambda_0$, $d = \lambda_0/5$, and $\nu = 0.1\Gamma_0$. (d) The field intensity in the xy plane with $z = 2.5\lambda_0$.

below the single atom decay rate. Therefore, it can be viewed as a minimal implementation of a laser. The collective nature of the dipole-dipole couplings leads to strong quantum correlations within the atoms and an inherent emission of a coherent field. Optimal operation is achieved when the collective state in the ring atoms features a single subradiant excitation only.

Model.—We consider N identical two-level atoms with states $|e\rangle$ and $|g\rangle$ each, separated by ω_0 and arranged in a ring geometry at an interatomic distance of $d \lesssim \lambda_0 = 2\pi c/\omega_0$. An additional gain atom is placed in the center of the ring as depicted in Fig. 1(a) and is assumed to be pumped to its upper level incoherently at a rate ν. The corresponding raising (lowering) operators of the ith atom are $\sigma_i^{\pm}$ for $i \in \{1, 2, \ldots, N, p\}$ (the index p corresponds to the central, pumped atom). The excited state is subject to spontaneous emission with a rate Γ_0. All transition dipoles $\boldsymbol{\mu}_i$ are chosen such that they point in the z direction.

This results in an effective dipole-dipole interaction [25], so that the atomic ring acts like a resonator [18] coupled to the gain atom in its center.

Using standard quantum optical techniques [27], we obtain a master equation for the dynamics, $\dot{\rho} = i[\rho, H] + \mathcal{L}_{\Gamma}[\rho] + \mathcal{L}_{\nu}[\rho]$, where the incoherent pumping of the central atom is given by $\mathcal{L}_{\nu}[\rho] = (\nu/2)(2\sigma_p^+\rho\sigma_p^- - \sigma_p^-\sigma_p^+\rho - \rho\sigma_p^-\sigma_p^+)$. The Hamiltonian in the interaction picture reads

$$H = \sum_{i,j: i \neq j} \Omega_{ij}\sigma_i^+\sigma_j^-, \qquad (1)$$

while the Lindblad operator accounting for collective spontaneous emission reads

$$\mathcal{L}_{\Gamma}[\rho] = \sum_{i,j} \frac{\Gamma_{ij}}{2}(2\sigma_i^-\rho\sigma_j^+ - \sigma_i^+\sigma_j^-\rho - \rho\sigma_i^+\sigma_j^-). \qquad (2)$$

The collective coupling rates Ω_{ij} and Γ_{ij} are given by the overlap of the transition dipole of the ith atom with the electric field emitted by the jth atom [28]. We compute the emitted field intensity [28] as

$$I(\boldsymbol{r}) = \langle \boldsymbol{E}^+(\boldsymbol{r})\boldsymbol{E}^-(\boldsymbol{r}) \rangle, \qquad (3)$$

The steady-state intensity is shown in Figs. 1(c) and 1(d) for typical operating conditions.

Continuous collective emission.—Our goal is to find operating regimes where the system emits coherent light with a narrow linewidth. As the configuration is rotationally symmetric, we can expect the ring atoms to be driven into a symmetric excitation state given as

$$|\psi_{\text{sym}}\rangle = \frac{1}{\sqrt{N}} \sum_{j=1}^{N} \sigma_j^+ |g\rangle^{\otimes N}. \qquad (4)$$

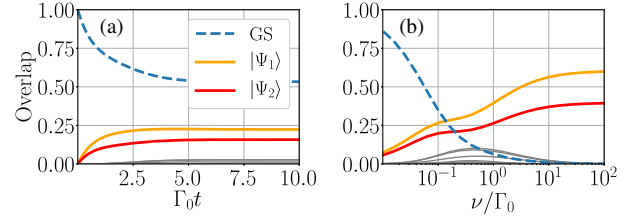In accordance with standard laser theory, we target parameters for which a symmetric excitation of the ring

FIG. 2. Dissipative system dynamics. (a) Time evolution of the eigenstates of the Hamiltonian from Eq. (1) for $N = 5$ ring atoms with an interatomic distance $d = \lambda_0/2$ and an incoherent pump rate $\nu = \Gamma_0/2$ starting from the ground state (GS). The state $|\Psi_{1,2}\rangle$ features a large contribution from the symmetric state of the ring atoms $|\psi_{\text{sym}}\rangle$ and shows significantly higher populations than all other excited eigenstates (gray lines) at all times. (b) Stationary population of the eigenstates for different pump rates. We can see that, even for large pump rates $\nu > \Gamma_0$, the symmetric single-excitation states dominate.

atoms constitutes a good cavity. To this end, we study the stationary populations of different eigenstates of our Hamiltonian from Eq. (1) during a time evolution starting from the ground state as depicted in Fig. 2(a).

As shown in Fig. 2, we find that the two eigenstates involving the symmetric single-excitation state in the ring are occupied predominately at all times (except for the ground state). These states are given by

$$|\Psi_i\rangle = a_i|g\rangle^{\otimes N} \otimes |e\rangle + b_i|\psi_{\text{sym}}\rangle \otimes |g\rangle, \qquad (5)$$

for $i \in \{1, 2\}$, where a_i and b_i depend on the particular geometry with $|a_i|^2 + |b_i|^2 = 1$.

Note that the gain atom can only emit one photon at a time. Hence, the single-excitation manifold dominates the dynamics even for pump rates substantially larger than the single-atom decay rate. This is shown in Fig. 2(b), where we plot the occupation probability of different eigenstates at steady state as a function of ν.

The fact that the ring forms a resonator can be seen more clearly as follows. Let us assume that only the symmetric state in the ring is populated. Thus, we can rewrite the Hamiltonian in the subspace spanned by the ground and excited state of the gain atom in the center, as well as the ground state of the ring and its symmetric state obtaining [28]

$$H_{\text{sym}} = \Omega_{\text{sym}}\sigma_{\text{sym}}^+\sigma_{\text{sym}}^- + \sqrt{N}\Omega_{\text{p}}(\sigma_{\text{sym}}^+\sigma_p^- + \text{H.c.}), \qquad (6)$$

where $\Omega_{\text{sym}} = \sum_{j=2}^{N} \Omega_{1j}$ is the dipole energy shift of the symmetric state. Written like this, the Hamiltonian resembles the Jaynes-Cummings Hamiltonian with the ring taking on the role of the cavity mode. In this sense, the symmetric subspace lowering operator $\sigma_{\text{sym}}^- := |g\rangle^{\otimes N}\langle\psi_{\text{sym}}| \otimes \mathbb{1}_p$ can be interpreted as the photon annihilation operator of our "cavity." The coupling between the gain atom and the cavity is then determined by Ω_p.
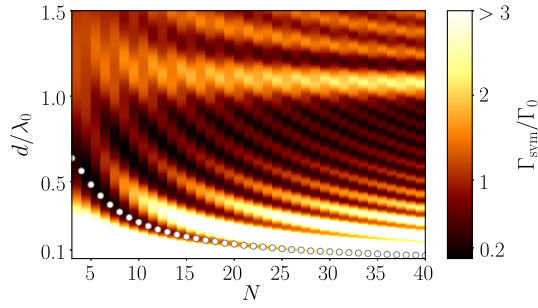
FIG. 3. Super- and subradiance of the symmetric state. The decay rate of the symmetric state Γ_{sym} as a function of the atom number in the ring and their interatomic distance. The white dots highlight specific interatomic distances where the decay of the symmetric state is the smallest (subradiant).

If we neglect the dissipative coupling between the central atom and the atoms forming the ring, i.e., $\Gamma_p = 0$, we can rewrite the decay of the system as $\mathcal{L}[\rho] = \mathcal{L}_\nu[\rho] + \mathcal{L}_0[\rho] + \mathcal{L}_{\text{sym}}[\rho]$, with

$$\mathcal{L}_0[\rho] = \frac{\Gamma_0}{2}(2\sigma_p^-\rho\sigma_p^+ - \sigma_p^+\sigma_p^-\rho - \rho\sigma_p^+\sigma_p^-), \tag{7a}$$

$$\mathcal{L}_{\text{sym}}[\rho] = \frac{\Gamma_{\text{sym}}}{2}(2\sigma_{\text{sym}}^-\rho\sigma_{\text{sym}}^+ - \sigma_{\text{sym}}^+\sigma_{\text{sym}}^-\rho - \rho\sigma_{\text{sym}}^+\sigma_{\text{sym}}^-). \tag{7b}$$

Minimizing the decay rate of the ring atoms is important, but in order to build up population within the ring, we need an efficient coupling to the gain atom as well. In analogy to the Jaynes-Cummings model, we define a cooperativity parameter [28] $C := N\Omega_p^2/(\Gamma_0\Gamma_{\text{sym}})$. An efficient coherent coupling of the ring atoms to the gain atom is achieved when $C > 1$. As we can see in Fig. 4(b), we reach this limit at extremely small distances or at a distance where Γ_{sym} is minimal (see Fig. 3). The cooperativity becomes large at $d < 0.1\lambda_0$ since, for $d \to 0$, the coherent coupling diverges. Yet, this is also the limit where the energy difference Ω_{sym} is large, which detunes the ring atoms from the gain atom. Furthermore, due to the superradiant loss of the ring in this limit, the emitted light features thermal statistics rather than coherence. Consequently, we find that the optimal parameter regime, indeed, lies where the ring atoms show a subradiant behavior, i.e., at the points highlighted in Fig. 3.

As seen in Fig. 4(a), the dissipative coupling of the central atom vanishes at points where the symmetric state shows suppressed spontaneous emission (white dots). Hence, the loss during the excitation transport from the gain medium to the ring is reduced as well. Note that it is important to distinguish the dissipative coupling from a physical decay rate: pairwise couplings can become negative, yet any collective state decays with a positive rate [25].

Photon statistics and spectral properties.—We have now identified a regime where our system resembles the typical
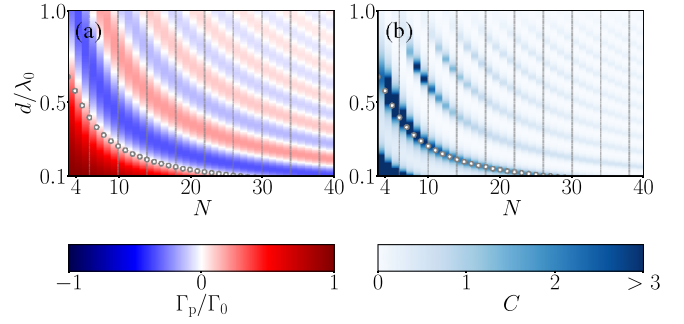

FIG. 4. Coupling of the central gain atom to the outer ring. (a) The dissipative coupling Γ_p between the central atom and the ring atoms as a function of the atom number N and the interatomic distance d. One can see that it becomes negligible at the points where $|\psi_{\text{sym}}\rangle$ is subradiant (white dots). (b) Cooperativity C for different distances and atom numbers. The cooperativity is large when $d \to 0$ due to the divergent behavior of Ω_p, or when Γ_{sym} is small.

setup of a single-atom laser. In order to study the statistical properties of the emitted light we calculate the normalized second-order correlation at zero time delay $g^{(2)}(0)$ of the electric field intensity. In the far-field, $r \gg \lambda_0$, where the intensity correlation function becomes independent of the position [28] and is given by

$$g^{(2)}(0) = \frac{\sum_{ijkl}\langle\sigma_i^+\sigma_j^+\sigma_k^-\sigma_l^-\rangle}{|\sum_{mn}\langle\sigma_m^+\sigma_n^-\rangle|^2}. \tag{8}$$

Coherent light exhibits a Poissonian statistic implying $g^{(2)}(0) = 1$ [27,33]. In addition, we calculate the amount of emitted light, i.e., $I_{\text{out}} := \sum_{ij}\Gamma_{ij}\langle\sigma_i^+\sigma_j^-\rangle$.

In Fig. 5(a), we can see that points of coherent light emission where $g^{(2)}(0) = 1$ are achieved along a curve strongly resembling the optimal subradiance parameters shown in Fig. 3. The points where $g^{(2)}(0) = 0$ correspond to the situation where the gain atom decouples from the cavity atoms, since then, only the single atom in the center can emit light, and we observe antibunching. However, this regime does not coincide with "lasing," since the ring atoms are not occupied. Simultaneously, the intensity shown in Fig. 5(b) is small, but still finite when the emitted light is coherent. This is because coherences can only build up when the loss from the atoms in the ring is sufficiently low (Γ_{sym} is small), which also reduces the amount of light emitted. Note, also, that our system behaves more like a superradiant laser than a conventional one. Such superradiant lasers exhibit an inherently small photon number [13]. Similarly, typical single-atom lasers also have weak output powers [2,34].

In order to analyze the emitted light in more detail, we compute its spectral linewidth. Therefore, we calculate the emission spectrum by means of the Wiener-Khinchin theorem [28,35]. It is given as the Fourier transform of
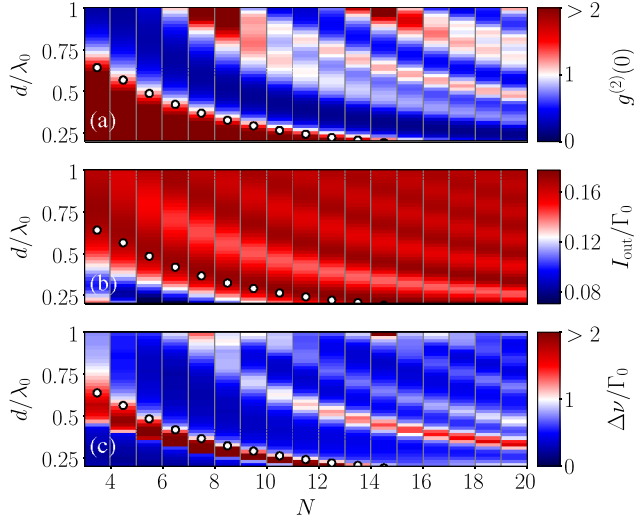
FIG. 5. Intensity and statistics of the emitted light. (a) Steady-state second-order correlation as a function of the ring atom number and atom spacing. For each atom number N there are specific interatomic distances d where the emitted light changes from thermal-like light emission (red), passing over regions of Poissonian statistics (white), to sub-Poissonian properties (blue). (b) The radiated intensity I_{out} for the same parameter region. Where $g^{(2)}(0) = 1$ the intensity is maximal, regardless of the atom number. (c) The spectral linewidth $\Delta\nu$ for the same parameters. It reduces to well below Γ_0. The pump rate was $\nu = 0.1\Gamma_0$. As before, the white dots indicate subradiance of the symmetric state.

the first-order coherence function, $g^{(1)}(\tau) := \sum_{i,j} \langle \sigma_i^+(\tau)\sigma_j^- \rangle$. The spectrum has a Lorentzian shape, thus, we compute the linewidth $\Delta\nu$ as the FWHM. In Fig. 5(c), we show the linewidth as a function of N and the interatomic distance d. Once again, we find that the linewidth is small ($\Delta\nu < \Gamma_0$) at the points where the symmetric state is subradiant. It can be seen that, in order to maintain coherent light emission, the interatomic distances need to become smaller for an increasing number of atoms in a ring of constant radius.

Note that, in order to treat larger atom numbers in the above calculations, we have truncated the Hilbert space at the second-excitation manifold [28]. Since the single-excitation subspace usually dominates (as shown in Fig. 2), neglecting any state containing more than two excitations is well justified.

On the one hand, comparing the linewidth shown here to the typical linewidth of a conventional laser as given by the Schawlow-Townes limit [36] is difficult. In order to obtain such a limit, one would need to linearize the system around a large classical field amplitude, which our system does not have. A similar approximation may be possible for very high atom numbers, but this would go beyond the scope of this Letter. On the other hand, as we have mentioned before, our system behaves more like a superradiant laser. This is also true for the linewidth of the emitted light in that it is determined by the linewidth of the atoms rather than an optical resonator.
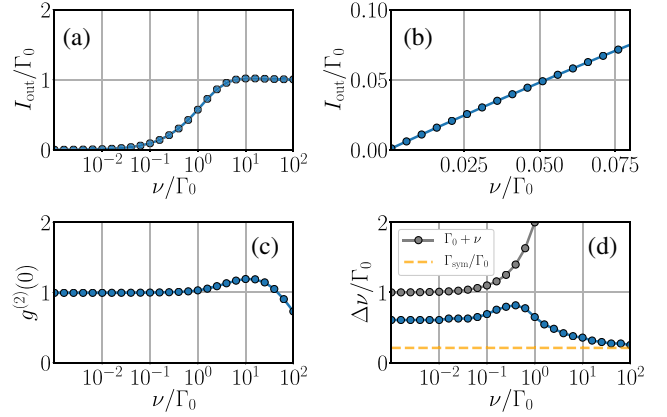

FIG. 6. Thresholdless coherent light emission. (a) I_{out} as a function of the pump rate ν for $N = 5$, $d = \lambda_0/2$ exhibiting a maximum from $\nu \approx 4\Gamma_0$ onwards. (b) A zoom in to the weak pump region shows the immediate onset of the intensity I_{out} at small ν. (c) The second-order correlation $g^{(2)}(0)$ in steady state is 1 for finite, but small ν. (d) The radiative linewidth $\Delta\nu$ (blue) in the steady state stays well below the pump broadened linewidth $\Gamma_0 + \nu$ of a single emitter (gray), and approaches the decay rate Γ_{sym} of the symmetric state (yellow, dashed line).

Thresholdless behavior.—In standard lasing models, coherent output light is achieved from a certain input power threshold on. Above threshold, the intensity of the emitted light increases drastically. In an effort to identify such a threshold in our setup, we compute the properties of the output light as a function of the pump strength of the gain atom.

The system does not exhibit a threshold. Such a thresholdless behavior has been observed in single-atom lasing setups [2]. As we can see in Figs. 6(a) and 6(b), the output intensity grows as soon as the pump rate becomes nonzero. At the same time, the photon statistics of the emitted field are Poissonian, i.e., $g^{(2)}(0) = 1$, for arbitrarily low pumping rates [see Fig. 6(c)]. The only point at which the photon statistics change is when the pump rate becomes large, $\nu \sim 10\Gamma_0$, such that the emitted light starts to reproduce the statistics of the input field. It can also be seen in Fig. 6(a) that above this point, the output intensity is reduced. As one would expect, the linewidth of the emitted field is small ($\Delta\nu < \Gamma_0$) as long as the light is coherent [see Fig. 6(d)]. When the incoherent pumping rate ν is increased, states outside the symmetric subspace are occupied, which leads to a slight increase in the linewidth. However, by increasing ν further, the linewidth decreases again and approaches Γ_{sym}, as the central atom decouples from the ring atoms, the light is emitted from the ring in the subradiant symmetric state.

Conclusions.—We predict that a continuously pumped single atom surrounded by a nanoring of identical atoms could act as a minimal, subwavelength sized implementation of a laser. Under suitable operating conditions, the system will emit spatially and temporally coherent light

with Poisson statistics. Our analysis reveals a close analogy to the Jaynes-Cummings model, where the outer ring atoms take on the role of a high-Q cavity mode with the central atom providing for gain. The system works best when driven into a collective subradiant state with a single excitation. In this limit, spontaneous emission is suppressed and the operation strongly resembles the behavior of a thresholdless laser [37]. While the implementation of such a system in a pure form could be envisioned in optical tweezer arrays of neutral atoms [21], analogous setups based on quantum dots have been implemented and are already operational in the pulsed excitation regime [38].

There are no principal lower physical limits on the size of the system apart from the technical implementation of the structure and its pumping. Hence, very high density arrays of such lasers on a surface are possible.

---

[*]raphael.holzinger@uibk.ac.at

[1] M. Brune, J. M. Raimond, P. Goy, L. Davidovich, and S. Haroche, Phys. Rev. Lett. **59**, 1899 (1987).

[2] J. McKeever, A. Boca, A. D. Boozer, J. R. Buck, and H. J. Kimble, Nature (London) **425**, 268 (2003).

[3] L. Davidovich, J. M. Raimond, M. Brune, and S. Haroche, Phys. Rev. A **36**, 3771 (1987).

[4] H. Walther, Phys. Scr. **T23**, 165 (1988).

[5] K. An, J. J. Childs, R. R. Dasari, and M. S. Feld, Phys. Rev. Lett. **73**, 3375 (1994).

[6] O. Astafiev, K. Inomata, A. Niskanen, T. Yamamoto, Y. A. Pashkin, Y. Nakamura, and J. S. Tsai, Nature (London) **449**, 588 (2007).

[7] G. Rastelli and M. Governale, Phys. Rev. B **100**, 085435 (2019).

[8] M. Löffler, G. M. Meyer, and H. Walther, Phys. Rev. A **55**, 3923 (1997).

[9] D. Meschede, H. Walther, and G. Müller, Phys. Rev. Lett. **54**, 551 (1985).

[10] Y. Mu and C. M. Savage, Phys. Rev. A **46**, 5944 (1992).

[11] T. Pellizzari and H. Ritsch, J. Mod. Opt. **41**, 609 (1994).

[12] T. Salzburger, P. Domokos, and H. Ritsch, Phys. Rev. A **72**, 033805 (2005).

[13] D. Meiser, J. Ye, D. R. Carlson, and M. J. Holland, Phys. Rev. Lett. **102**, 163601 (2009).

[14] D. Meiser and M. J. Holland, Phys. Rev. A **81**, 033847 (2010).

[15] S. Bedoui, M. Lopes, W. Nicolazzi, S. Bonnet, S. Zheng, G. Molnár, and A. Bousseksou, Phys. Rev. Lett. **109**, 135702 (2012).

[16] T. Maier, S. Krämer, L. Ostermann, and H. Ritsch, Opt. Express **22**, 13269 (2014).

[17] C. Hotter, D. Plankensteiner, L. Ostermann, and H. Ritsch, Opt. Express **27**, 31193 (2019).

[18] M. Moreno-Cardoner, D. Plankensteiner, L. Ostermann, D. E. Chang, and H. Ritsch, Phys. Rev. A **100**, 023806 (2019).

[19] M. Manzoni, M. Moreno-Cardoner, A. Asenjo-Garcia, J. V. Porto, A. V. Gorshkov, and D. Chang, New J. Phys. **20**, 083048 (2018).

[20] K. E. Ballantine and J. Ruostekoski, Phys. Rev. Research **2**, 023086 (2020).

[21] D. Barredo, S. de Léséleuc, V. Lienhard, T. Lahaye, and A. Browaeys, Science **354**, 1021 (2016).

[22] D. Barredo, V. Lienhard, S. de Léséleuc, T. Lahaye, and A. Browaeys, Nature (London) **561**, 79 (2018).

[23] Y. Wang, S. Shevate, T. M. Wintermantel, M. Morgado, G. Lochead, and S. Whitlock, arXiv:1912.04200.

[24] A. Blais, R.-S. Huang, A. Wallraff, S. M. Girvin, and R. J. Schoelkopf, Phys. Rev. A **69**, 062320 (2004).

[25] R. Lehmberg, Phys. Rev. A **2**, 883 (1970).

[26] J. D. Hood, A. Goban, A. Asenjo-Garcia, M. Lu, S.-P. Yu, D. E. Chang, and H. Kimble, Proc. Natl. Acad. Sci. U.S.A. **113**, 10507 (2016).

[27] C. Gardiner and P. Zoller, *Quantum Noise: A Handbook of Markovian and Non-Markovian Quantum Stochastic Methods With Applications to Quantum Optics* (Springer Science & Business Media, Berlin, 2004).

[28] See Supplemental Material at http://link.aps.org/supplemental/10.1103/PhysRevLett.124.253603 for a discussion of the Green's Function, the symmetric subspace and the scaling behavior, which includes Refs. [29–32].

[29] J. D. Jackson, *Classical Electrodynamics* (John Wiley & Sons, New York, 2007).

[30] A. Asenjo-Garcia, M. Moreno-Cardoner, A. Albrecht, H. J. Kimble, and D. E. Chang, Phys. Rev. X **7**, 031024 (2017).

[31] A. Asenjo-Garcia, J. D. Hood, D. E. Chang, and H. J. Kimble, Phys. Rev. A **95**, 033818 (2017).

[32] H. Carmichael, *An Open Systems Approach to Quantum Optics: Lectures Presented at the Université Libre de Bruxelles* (Springer Science & Business Media, Berlin, 1991).

[33] L. Mandel and E. Wolf, *Optical Coherence and Quantum Optics* (Cambridge University Press, Cambridge, England, 1995).

[34] F. Dubin, C. Russo, H. G. Barros, A. Stute, C. Becher, P. O. Schmidt, and R. Blatt, Nat. Phys. **6**, 350 (2010).

[35] H. Carmichael, *An Open Systems Approach to Quantum Optics: Lectures Presented at the Université Libre de Bruxelles, 1991* (Springer Science & Business Media, Berlin, 2009), Vol. 18.

[36] A. L. Schawlow and C. H. Townes, Phys. Rev. **112**, 1940 (1958).

[37] A. Boca, R. Miller, K. M. Birnbaum, A. D. Boozer, J. McKeever, and H. J. Kimble, Phys. Rev. Lett. **93**, 233603 (2004).

[38] B. le Feber, F. Prins, E. De Leo, F. T. Rabouw, and D. J. Norris, Nano Lett. **18**, 1028 (2018).

[39] S. Krämer, D. Plankensteiner, L. Ostermann, and H. Ritsch, Comput. Phys. Commun. **227**, 109 (2018).

[40] J. D. Hunter, Comput. Sci. Eng. **9**, 90 (2007).